

R. G. Berman · L. Ya Aranovich · D. R. M. Pattison

Reassessment of the garnet-clinopyroxene Fe-Mg exchange thermometer: II. Thermodynamic analysis

Received: 3 September 1993 / Accepted: 16 June 1994

Abstract The garnet (Grt)-clinopyroxene (Cpx) Fe-Mg exchange thermometer has been re-evaluated through analysis of phase equilibrium experiments defining the Fe-Mg exchange between Grt and Cpx, Grt and Ol (Ol = Olivine), and Cpx and Ol, together with thermophysical and other phase equilibrium constraints on solid solution and individual end-member properties. Results show that all data are mutually compatible if the heterogeneity range of Grt and Cpx in run products previously obtained by Pattison and Newton (PN) are accounted for in assessing equilibrium Grt-Cpx compositions. Derived mixing properties are in good agreement with results from numerous recent phase equilibrium studies. Application of the newly calibrated thermometer to a number of amphibolite to granulite facies terrains indicates temperatures between 70 and 200 °C above PN's thermometer, and general compatibility with independent temperature estimates.

Introduction

This paper is Part II of a two-part study on the garnet (Grt)-clinopyroxene (Cpx) Fe-Mg exchange equilibrium:



(see Table 1 for abbreviations). This equilibrium is one of the most important geothermometers for am-

phibolite-granulite facies mafic and ultramafic rocks (e.g. Perchuk 1969; Råheim and Green 1974; Ellis and Green 1979; Saxena 1979; Ganguly 1979; Dahl 1980; Powell 1985a; Pattison and Newton 1989; Green and Adam 1991). Equilibrium (A) has been calibrated experimentally on the basis of four different studies investigating the compositions of coexisting Grt and Cpx at high *P-T* (Råheim and Green 1974; Ellis and Green 1979; Pattison and Newton 1989; Green and Adam 1991). Of these studies, only one was designed to obtain compositional constraints on the exchange reaction using crystalline starting materials of a wide range in bulk composition (Pattison and Newton 1989). Two controversial results of this study were that:

(1) their nominal experimental results were inconsistent with any previously proposed garnet and clinopyroxene solution models, and their derived geothermometer contained terms indicative of strong nonideality in either or both of the solid solutions;

(2) their formulation of the Grt-Cpx thermometer produced temperature estimates for many terrains which in most cases were significantly lower than previous calibrations, and which clustered at or below the low temperature limit imposed by other geothermometers, petrogenetic grids and/or "petrological intuition" (e.g. see Table 6 of Pattison and Newton 1989).

These results have led some petrologists to question the ability of Fe-Mg exchange thermometers to record near-peak metamorphic conditions for relatively high-grade rocks (e.g. Pattison & Newton 1989; Frost and Chacko 1989). The Pattison and Newton (1989) results have additionally stimulated other experimental studies (e.g. Perkins and Vielzeuf 1992; Kawasaki and Ito 1993) involving Cpx and/or Grt solid solutions in order to test the findings of Pattison and Newton (1989). Perkins and Vielzeuf (1992) concluded that their experimental results for the Ol-Cpx exchange equilibrium, combined with those of Hackler and Wood (1989) for the Ol-Grt exchange equilibrium, are inconsistent with those of Pattison and Newton (1989) unless

R. G. Berman (✉)
Geological Survey of Canada, 601 Booth St., Ottawa, Ontario,
Canada K1A 0E8

L. Ya Aranovich
Institute of Experimental Mineralogy, Chernogolovka, Russia

D. R. M. Pattison
Department of Geology and Geophysics, University of Calgary,
Calgary, Alberta T2N 1N4, Canada

Editorial responsibility: K. Hodges

Table 1 Abbreviations of phases and components

Phase/ Component	Abbreviation	Formula
Garnet	Grt	(Ca, Mg, Fe) ₃ Al ₂ Si ₃ O ₁₂
Grossular	Gr	Ca ₃ Al ₂ Si ₃ O ₁₂
Pyrope	Py	Mg ₃ Al ₂ Si ₃ O ₁₂
Almandine	Alm	Fe ₃ Al ₂ Si ₃ O ₁₂
Clinopyroxene	Cpx	(Ca, Mg, Fe, Na)(Mg, Fe, Al) (Al, Si) ₂ O ₆
Diopside	Di	CaMgSi ₂ O ₆
Hedenbergite	Hd	CaFeSi ₂ O ₆
Olivine	Ol	(Mg, Fe) ₂ SiO ₄
Forsterite	Fo	Mg ₂ SiO ₄
Fayalite	Fa	Fe ₂ SiO ₄

uncertainties in one or more of the experimental data sets were underestimated. Perkins and Vielzeuf (1992) reported that their formulation of the Grt-Cpx thermometer yields temperature estimates about 30–190°C higher than that of Pattison and Newton (1989).

In this paper we present the results of a thermodynamic analysis of the phase equilibrium data of Pattison and Newton (1989; PN). These data are critically re-evaluated in Part I of this study (Aranovich and Pattison 1994). Additional Fe-Mg exchange equilibrium data involving clinopyroxene, garnet, and olivine, as well as thermophysical data are used to constrain the thermodynamic properties of end-members and mixing properties of Grt, Cpx, and Ol solid solutions. The primary motivation of this study is not to derive comprehensive thermodynamic models for these phases, but to answer the questions whether reasonable thermodynamic properties can be derived that satisfy all experimental observations *within their uncertainties*, and, if so, whether the low-temperature estimates for many amphibolite and granulite facies rocks found by Pattison and Newton (1989) are dictated by their experimental data.

Thermodynamic model

For (A), the thermodynamic requirement for equilibrium can be expressed as:

$$\Delta_r G^{P,T} = -RT \ln K = -RT \ln \frac{a_{Alm} \cdot a_{Di}^3}{a_{Py} \cdot a_{Hd}^3} = -3RT \ln K_D - 3RT \ln K_y \quad (1)$$

with

$$K_D = \frac{X_{Fe}^{Grt} X_{Mg}^{Cpx}}{X_{Mg}^{Grt} X_{Fe}^{Cpx}} \quad (2)$$

and

$$3RT \ln K_y = \Delta G_{ex} = 3RT \ln \frac{\gamma_{Fe}^{Grt} \cdot \gamma_{Di}}{\gamma_{Mg}^{Grt} \cdot \gamma_{Hd}} \quad (3)$$

$\Delta_r G^{P,T}$ is the change in standard Gibbs free energy of reaction which can be expressed as:

$$\begin{aligned} \Delta_r G^{P,T} = & \Delta_r H^0 - T \Delta_r S^0 + \int_{298.15}^T \Delta C_p dT \\ & - T \int_{298.15}^T \frac{\Delta C_p}{T} dT + (P-1) \Delta_r V^0 \\ & + \int_1^P (\Delta_r V^{P,T} - \Delta_r V^0) dP \end{aligned} \quad (4)$$

with $\Delta_r H^0$, $\Delta_r S^0$, and $\Delta_r V^0$ being the standard reaction properties at 1 bar and 25°C. Expansion of the heat capacity and volume integrals are given in Berman (1988). ΔG_{ex} represents the change in excess Gibbs free energy for equilibrium (A). In order to evaluate the ΔG_{ex} term of Eq. 3 and analogous equations involving equilibria with olivine, our assumptions regarding solid solution models are discussed below.

Olivine

Fe-Mg mixing in olivine has been the subject of considerable experimental investigation. Sack and Ghiorso (1989) found that available calorimetric data were most compatible with a symmetric regular solution parameter (W_H) equal to 20.3 kJ/4 oxygen formula. More recent studies based on various phase equilibria indicate values in the range 7–10 kJ/4 oxygen basis, with excess entropy less than 4 J/K.4 oxygen basis (e.g. Hackler and Wood 1989; Wisser and Wood 1991; von Seckendorff and O'Neill 1993). In this study we allowed the mixing properties of olivine to be variables determined by thermodynamic analysis of the combined experimental dataset. Due to very restricted Ca solubility in olivine at the conditions of experiments analysed in this study, Ca in olivine was ignored.

Garnet

As the experimental data considered in this study contain aluminosilicate garnet, we did not consider the substitution of trivalent cations (e.g. Cr, Fe³⁺) on the octahedral sites of garnet, restricting our attention to the mixing of Ca, Mg and Fe atoms on three energetically equivalent 8-fold positions. Garnet mixing properties on the grossular-almandine join are reasonably well constrained by both calorimetric and phase equilibrium studies (Geiger et al. 1987; Koziol 1990; Berman 1990). In contrast, the pyrope-grossular join is only loosely constrained by phase equilibrium data (Wood 1988) because of added experimental difficulties due to clinopyroxene stability in this system. Calorimetric measurements on this join (Newton et al. 1977) indicate more positive excess enthalpy in Gr-poor

compositions, whereas interpretation of recent X-ray and ternary garnet phase equilibrium data yield excess volumes and enthalpies with the opposite asymmetry (Cheng and Ganguly 1992). Mixing properties of almandine-pyrope solutions have been the subject of considerable debate (e.g. Aranovich 1983; Ganguly and Saxena 1984; Lee and Ganguly 1988; Sack and Ghiorso 1989; Hackler and Wood 1989; Berman 1990; Koziol and Bohlen 1992), with the weight of recent experimental data favouring near-ideal behaviour. These studies also suggest slightly larger excess enthalpies in Fe-rich compositions, the asymmetry in enthalpy mimicking that in excess volumes. In order not to bias unduly the results of this investigation of Grt-Cpx systematics by previous results, we determined garnet mixing properties, along with those of clinopyroxene and olivine, from available phase equilibrium, applying the subregular model for each binary garnet join.

Clinopyroxene

In the system $\text{Na}_2\text{O}-\text{CaO}-\text{FeO}-\text{MgO}-\text{Al}_2\text{O}_3-\text{SiO}_2$, clinopyroxene is a complex three-site solution with mixing of Na, Ca, Fe, Mg cations on the M2 site, Mg, Al, Fe on the M1 site, and Al and Si on the tetrahedral sites. Site occupancy data for Cpx show a strong partitioning of Fe into the larger M2 site, but uncertainties remain particularly with respect to the temperature and Ca dependence of Fe-Mg partitioning. These uncertainties are manifested in considerable disagreement between site occupancies measured experimentally (Brown et al. 1972; Saxena et al. 1974; McCallister et al. 1976) and those calculated with non-convergent ordering model parameters derived from phase equilibrium data (Davidson and Lindsley 1985; Sack and Ghiorso 1994). Early on in this study we investigated various temperature and compositionally dependent Fe-Mg partitioning schemes reported in the literature, and found that none allowed adequate representation of phase equilibrium data as well as models with no explicit account of Fe-Mg ordering. This suggests that available site occupancy data do not constrain ordering models with sufficient accuracy to accommodate the much wider range of temperature and compositions used in phase equilibrium studies compared to site occupancy measurements. In addition, deviations of Ca contents in Cpx from the Di-Hd join were not reported in one of the experimental studies utilized below (Kawasaki and Ito 1993). We therefore adopted a simplified model for clinopyroxene solid solution which assumes equal partitioning of Fe and Mg atoms between M2 and M1 sites and ignores possible cross-site interactions. We used an excess entropy of mixing term to indicate the deviation of the experimental clinopyroxenes from this equal partitioning reference state.

According to this model, the M1 site is treated as a ternary regular solution of Mg, Fe and Al atoms, and

the M2 site as a quaternary solution of Na, Ca, Fe and Mg atoms. $\text{Mg}/(\text{Mg} + \text{Fe})$ is assumed equal in both M1 and M2. Mixing on the tetrahedral site of Cpx is assumed to be ideal and coupled to octahedral site substitutions (e.g. Newton 1983). The effect of variable Na in run products of Pattison and Newton (1989) was empirically accounted for by adding to the M1 site the amount of Al necessary to balance Na on the M2 site, giving: $\text{Al}^{\text{M1}} = \text{Na} + (\text{Al} - \text{Na})/2$. Substituting $\gamma_{\text{Hd}} = \gamma_{\text{FeM1}}^{\text{Cpx}} \cdot \gamma_{\text{CaM2}}^{\text{Cpx}}$ and $\gamma_{\text{Di}} = \gamma_{\text{MgM1}}^{\text{Cpx}} \cdot \gamma_{\text{CaM2}}^{\text{Cpx}}$ into Eq. 3 yields:

$$\Delta G_{\text{ex}} = 3RT \ln \frac{\gamma_{\text{Fe}}^{\text{Grt}} \cdot \gamma_{\text{MgM1}}^{\text{Cpx}} \cdot \gamma_{\text{CaM2}}^{\text{Cpx}}}{\gamma_{\text{Mg}}^{\text{Grt}} \cdot \gamma_{\text{FeM1}}^{\text{Cpx}} \cdot \gamma_{\text{CaM2}}^{\text{Cpx}}} = 3RT \ln \frac{\gamma_{\text{Fe}}^{\text{Grt}} \cdot \gamma_{\text{MgM1}}^{\text{Cpx}}}{\gamma_{\text{Mg}}^{\text{Grt}} \cdot \gamma_{\text{FeM1}}^{\text{Cpx}}} \quad (5)$$

Note that M2 site interactions in Cpx cancel for the exchange equilibrium (Δ) as long as mixing on M1 and M2 is assumed to be independent. Substituting the generalized Margules equation of Berman (1990) for Eq. 5 gives:

$$\begin{aligned} \Delta G_{\text{ex}} = & 3W_{12}^{\text{Cpx}}(Y_2 - Y_1) + 3(W_{13}^{\text{Cpx}} - W_{23}^{\text{Cpx}})Y_3 \\ & - W_{112}^{\text{Gt}}(X_1^2) - W_{122}^{\text{Gt}}(2X_1X_2) + W_{113}^{\text{Gt}}(X_1^2) \\ & + W_{133}^{\text{Gt}}(2X_1X_3) + W_{223}^{\text{Gt}}(X_2^2 - 2X_2X_3) \\ & + W_{233}^{\text{Gt}}(2X_2X_3 - X_3^2) - W_{123}^{\text{Gt}}(X_1X_3 - X_1X_2) \end{aligned} \quad (6)$$

where X is the mole fraction of eight-coordinated cations in Grt (1 = Ca, 2 = Mg, 3 = Fe) and Y is the mole fraction of cations on the M1 site of Cpx (1 = Mg^{M1} , 2 = Fe^{M1} , 3 = Al^{M1}). The temperature and pressure dependence of ΔG_{ex} can be expressed as

$$\Delta G_{\text{ex}} = \Delta H_{\text{ex}} - T\Delta S_{\text{ex}} + (P - 1)\Delta V_{\text{ex}} \quad (7)$$

Similarly, W terms in Eq. 6 may be replaced by $[W_{\text{H}} - TW_{\text{S}} + (P - 1)W_{\text{V}}]$.

Combination of Eqs. 1-7, while omitting heat capacity, expansivity, and compressibility terms, yields the standard equation of a geothermometer:

$$T = \frac{-\Delta_r H - (P - 1)(\Delta_r V + \Delta V_{\text{ex}}) - \Delta H_{\text{ex}}}{3R \ln K_{\text{D}} - \Delta_r S - \Delta S_{\text{ex}}} \quad (8)$$

Measured mineral compositions giving K_{D} are combined with known thermodynamic parameters to solve Eq. 8 for T (in Kelvins) at a given P (in bars).

In order to derive thermodynamic parameters, experimental values of P and T are combined with measured mineral compositions. In this study we have derived garnet, clinopyroxene, and olivine mixing properties and end-member properties from analysis of selected phase equilibrium data, combined with calorimetric (C_p , S) and volumetric (V , α , β) constraints on end-member properties. The standard state properties of all Mg end-members were taken from Berman (1988). Because the uncertainties associated with calorimetrically determined heats of solution do not provide precise enough constraints (Aranovich 1991; Berman 1988), phase equilibrium data were used to

Table 2 Phase equilibrium data used in thermodynamic analysis (compositional uncertainties are estimated values used in thermodynamic analysis unless marked with asterisk; see text for discussion. System: *exch* Fe-Mg exchange reaction, *F* FeO, *S* SiO₂, *A* Al₂O₃, *T* TiO₂, *C* CaO)

#	Equilibrium	System	Uncertainties		Authors
(A)	3 hedenbergite + pyrope = almandine + 3 diopside	exch	0.015 Cpx, Grt*	5° C, 1 kbar	Pattison Newton (1989), Aranovich Pattison (1994)
(B)	forsterite + 2 hedenbergite = fayalite + 2 diopside	exch	0.010Ol, Cpx 0.015Ol, Cpx 0.015Ol, Cpx	5° C, 1 kbar 15° C, 2 kbar 20° C, 5 kbar	Perkins Vielzeuf (1992) Kawasaki Ito (1993) @ 27 kbar Kawasaki Ito (1993) @ 68 kbar
(C)	3fayalite + 2 pyrope = 2almandine + 3 forsterite	exch	0.010Ol, Grt	5° C, 1 kbar	Hackler Wood (1989)
(D)	3anorthite = grossular + 2kyanite + quartz	Gr-Alm Gr-Py	0.010 Grt 0.010 Grt	5° C, 0.5 kbar 5° C, 1 kbar	Koziol (1990) Wood (1988)
(E)	3fayalite + 3 anorthite = grossular + 2 almandine	Gr-Alm	0.010 Grt	5° C, 0.3 kbar	Bohlen et al. (1983b)
(F)	3ilmenite + sillimanite + quartz = almandine + 3 rutile	Py-Alm	0.010 Grt	5° C, 0.3 kbar	Koziol and Bohlen (1992)
(G)	6ilmenite + 3 anorthite + 3 quartz = grossular + rutile + 2 almandine	CFAST		5° C, 0.3 kbar	Bohlen and Liotta (1986)
(H)	2 ferrosilite = fayalite + quartz	FS		5° C, 0.3 kbar	Bohlen et al. (1980)
(I)	3ilmenite + sillimanite + quartz = almandine + 3 rutile	FAST		5° C, 0.3 kbar	Bohlen et al. (1983a)

determine enthalpies of formation of Fe end-members and mixing properties, although it should be noted that derived thermodynamic properties are strongly correlated. Net transfer equilibria that constrain thermodynamic properties of Cpx components (CaAl₂SiO₆, NaAlSi₂O₆, Mg₂Si₂O₆) other than those in equilibrium (A) were not considered because they serve largely to calibrate thermodynamic properties of these components, they are dependent on compositional parameters that were not explicitly investigated by PN, and they introduce ambiguities regarding M2 site interactions that cancel for equilibrium (A). We chose to adopt the simplest solution models that were consistent with the experimental data, so as to allow the best extrapolation from the experimental data to the range of bulk compositions found in nature.

For our analysis we used the method of linear programming (LIP) to solve the linear inequality constraints derived from Eq. (1) through consideration of the direction in which equilibrium compositions were assumed to be approached. LIP allows explicit incorporation of experimental uncertainties, and thus provides a direct answer to the question whether there is any combination of thermodynamic data capable of satisfying all experiments at a specified uncertainty level. If not, the experiments may have failed, uncertainties may have been underestimated, or more complex or different solution models may be required. Although application of LIP is straightforward for phase equilibria involving stoichiometric minerals (see Berman et al. 1986 for a detailed discussion), treatment

of equilibria involving solid solutions may be complicated by the occurrence of overlapping (apparently contradictory) half-brackets. This overlap may be caused by errors in measured compositions or by real overstepping of the equilibrium through nucleation and growth of new compositions (e.g. Pattison 1994). In any case, the amount of overlap gives a good approximation of the *minimum* uncertainties in determining equilibrium compositions. These are discussed further below in relation to each experimental study involving solid solution phases.

LIP is also suited to analysing data that constrain the position of an equilibrium using single rather than paired experiments over significant compositional ranges (e.g. the high pressure data for equilibrium B discussed below), subject to added uncertainties related to possible equilibrium overstepping. Regression analysis of such data suffers a related problem in that experimentally determined compositions may not have closely approached equilibrium.

Treatment of phase equilibrium data

Table 2 lists the sources of phase equilibrium data used to define garnet, clinopyroxene, and olivine properties, along with reported or assumed uncertainties. Data for equilibria (A-C) form the backbone of this study. Only two of these equilibria are linearly independent so that simultaneous analysis of all three sets of experimental constraints provides a stringent test of their compatibility. Experimental data for equilibria (D-G) constrain Grt solution properties on various binary joins as well as end-member properties, while data for

equilibria (H-I) constrain Fe end-member properties. Treatment of data for equilibria (D-I) follows that discussed by Berman (1988; 1990) and is not discussed further here.

Compositional uncertainties applied to each set of experimental data involving a solid solution phase are based on estimated minimum analytical errors of $Mg\# = Mg/(Mg + Fe) = \pm 0.01$. In some cases, overlapping half-brackets, after ± 0.01 compositional adjustment, suggest somewhat greater uncertainties due either to microprobe errors or real compositional heterogeneity. The latter source of uncertainty is discussed below for each set of experiments of equilibria (A-C).

Experiments for equilibrium (A)

Synthesis experiments on the Grt-Cpx equilibrium (Ellis and Green 1979; Green and Adam 1991) were not included in our analysis because of the difficulty in analysing single phases in the fine intergrowths produced in experiments, and estimating equilibrium compositions from the range of measured analyses when the direction of approach to equilibrium is not known and the starting materials (glasses) are highly metastable.

In order to minimize compositional change in Grt, PN used bulk ratios of Grt:Cpx = 95:5. Results of reanalysis of run products of more than half of PN's experiments on equilibrium (A) are presented in Part I of this study. This work confirmed most of the findings of the original PN study, including the presence of small but significant Na in most of the product Cpx, and Mg/(Mg + Fe) ratios for Grt and Cpx (with the exception of a few 1100 and 1200°C runs with Mg-rich starting garnet) similar to those reported by PN. The most important additional observation of Part I was that garnets in the run products displayed non-negligible compositional heterogeneity (.03 – .06 Mg/(Mg + Fe)), with a slight but irregular trend in core to rim zoning generally consistent with mass balance constraints. Grt in run products showed the same or larger heterogeneity range as that reported by PN for starting garnets (0.025 to 0.065 Mg/(Mg + Fe)) probably because more analyses of run products were collected. This wide heterogeneity range probably resulted from synthesis of garnets from mechanical mixtures of end-member glasses, and thus was present during exchange experiments. The implications for modelling these data are that the equilibrium Grt composition may not be known more closely than \pm one half of the heterogeneity range (see Part I).

An additional key observation discussed in Part I was that changes in Cpx composition during an experiment were produced by nucleation and growth of new Cpx, rather than diffusional re-equilibration of the starting Cpx. As such, the new compositions do not represent strict reversals or limiting brackets of equilibrium (A), a conclusion that may account for the large (0.02 – 0.06 Mg/(Mg + Fe)) "overlap" of Cpx compositions observed in ten pairs of experiments using Mg-rich and Fe-rich starting Cpx. In order to analyse these data, the sign of the inequality constraints was reversed, a technique also employed by Carlson & Lindsley (1988). This procedure, which forces the equilibrium position between the two paired experimental results, is not critical to this analysis because none of the ten pairs of experimental results were found to be as constraining as other PN experiments.

The above discussion suggests that minimum compositional uncertainties must be considerably greater than estimated 0.01 Mg/(Mg + Fe) analytical errors. For garnet, uncertainties were initially assumed to correspond to the range of compositions (both X_{Gr} and Mg#) measured either for the starting or product garnets. For Cpx, uncertainties were assumed to be 0.015 Mg/(Mg + Fe). With these assumptions, all the PN data are compatible with one another. LIP analysis revealed that all PN data could be internally consistent (when considered by themselves) with uncertainties in garnet compositions as small as 0.03 Mg#, a value very similar to the minimum garnet heterogeneity range reported by PN and in Part I.

Experiments for equilibrium (B)

Perkins and Vielzeuf (1992; PV) report results at 1000°C – 10.5 kbar over the compositional range Cpx Mg# = 0.05 – 0.95. Most synthetic olivines and clinopyroxenes were homogeneous to within 0.01–0.02 Mg#, with several intermediate Cpx compositions showing heterogeneities up to 0.03 Mg#. Experiments consisted of 95% Cpx – 5% O1 in order to minimize the amount of Ca transferred from Cpx to O1. For each of 15–30 olivine grains in each run product, 5–10 analyses of adjacent Cpx were collected. For each run, PV show the two or three pairs of Cpx and O1 compositions that indicate the largest change in K_D during the run, rejecting analyses with inferior stoichiometries or which showed signs of interference from the adjacent phase. Taken alone, these data are mutually consistent with 0.01 compositional uncertainties, although only marginally so because of the large apparent overlap of the most advanced (run product compositions) that yield K_D most different from starting compositions) Cpx-O1 pair (mixture P).

Kawasaki and Ito (1993; KI) present data for equilibrium (B) at 30 kbar (900 and 1100°C) and 75 kbar (1100, 1300, and 1500°C). Based on results presented by Perkins et al. (1981), we assumed a –3 kbar pressure correction for the lower pressure data which were collected in a piston cylinder apparatus with a talc-pyrex cell. Based on comparisons reported by Brey and Kohler (1990), we assumed a –7 kbar correction for the higher pressure data collected in a uniaxial split sphere apparatus. Temperature was controlled within 10°C during all experiments, but we expanded the temperature uncertainties to 20°C for the 75 kbar runs in order to account for the influence of very high pressure on the measured thermocouple EMF. Starting compositions were homogeneous to within 1–2 mol%. Runs in which either O1 or Cpx showed compositional heterogeneities greater than 0.03 Mg# were considered to have failed by Kawasaki and Ito (1993) and were not reported. Tabulated data appear to represent the most advanced compositions analysed in each run. Analysed by themselves, these data are inconsistent with 0.01 Mg# compositional uncertainties, due to fairly large compositional overlaps produced at several *P-T* conditions. All data are compatible, however, with 0.015 Mg# uncertainties.

Experiments for equilibrium (C)

Hackler and Wood (1989) present bracketed data at 1000°C and 9.1 kbar for equilibrium (C) with garnet Mg# = 0.17 – 0.67. Synthetic garnets and olivines were homogeneous to within 2.5 to 0.5 mol%, respectively. Experiments contained Grt:O1 ratios of 10:1 by weight in order to minimize compositional changes in Grt. Their tabulated analyses of run products include homogeneous olivine and the most advanced of the slight range of garnet compositions surrounding olivine. Final Grt compositions shifted in the expected direction from nominal starting compositions to compensate changes in O1 composition, but in only one experiment was the change in composition greater than the starting Grt heterogeneity range. These data are internally consistent using compositional uncertainties of 0.01.

Results

Having established minimum uncertainties for internal consistency of each of the experimental data sets considered alone, we analysed them in pairs using our estimates of uncertainties given in Table 2 and discussed above. Each experimental study is compatible with that of Hackler and Wood (1989), but some

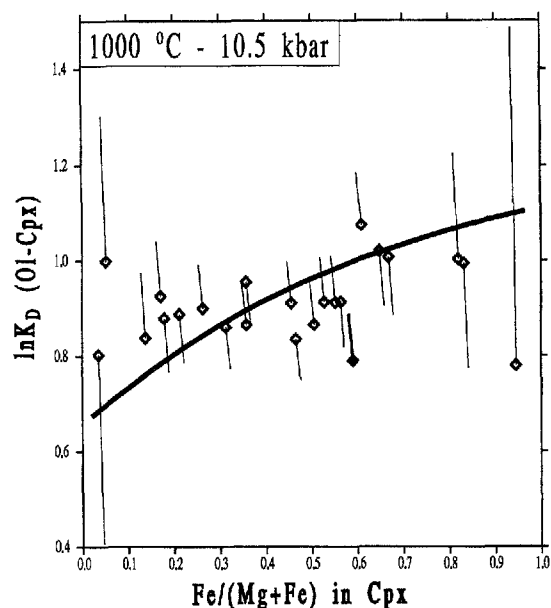


Fig. 1 Comparison of computed 10.5 kbar – 1000 °C $\ln K_D$ curve for equilibrium (B) with experimental data of Perkins and Vielzeuf (1992). Symbols with *connected lines* should be viewed as *arrows* (symbols are the *arrowheads*) indicating direction of $\ln K_D$ change during experiment. Lines on the high or low $\ln K_D$ side of symbols reflect whether $\ln K_D$ was experimentally approached from above or below, respectively. Symbols show most advanced $\ln K_D$ values based on nominal experimental data. *Length of connected lines* shows effect on $\ln K_D$ of 0.01 adjustment of the compositions of Ol and Cpx. Calculated $\ln K_D$ values that plot along the length of the arrows are inconsistent with nominal experimental data, but consistent with data adjusted for quoted uncertainties. Note that nominal data (symbols) suggest slightly flatter slope than calculated, and that one experimental datum (*highlighted in bold*) is inconsistent with the calculated equilibrium position *after adjustment for 0.01 uncertainties*

problems arise with all other combinations. All Ol-Cpx experiments are not consistent when analysed together, suggesting uncertainties for at least some experiments that are somewhat larger than assumed initially. The inconsistency arises mostly because the nominal PV data indicate an extremely flat slope for the dependence of K_D (Ol-Cpx) on $\text{Fe}/(\text{Fe} + \text{Mg})$ (Fig. 1), whereas the data of KI (Figs. 2 and 3) suggest a steeper slope, especially at 900 and 1100 °C. The inconsistency can be resolved by omitting one experiment of Perkins and Vielzeuf (1992; mixture P), or by omitting three experiments of Kawasaki and Ito (1993; runs # MSA9005231, KCH9009125, KCH900912B). The first option was adopted because the offending PV experiment is almost incompatible with other PV results when these data are treated alone (see Fig. 1). Results based solely on experiments for equilibrium (B) and (C) indicate positive excess free energies in Cpx at all temperatures, producing a maximum in a plot of $\ln K_D$ (Ol-Cpx) versus $\text{Fe}/(\text{Fe} + \text{Mg})$, as shown by Perkins and Vielzeuf (1992).

Analysis of all experiments for equilibria (A-C) except the PV run described above, led to small incom-

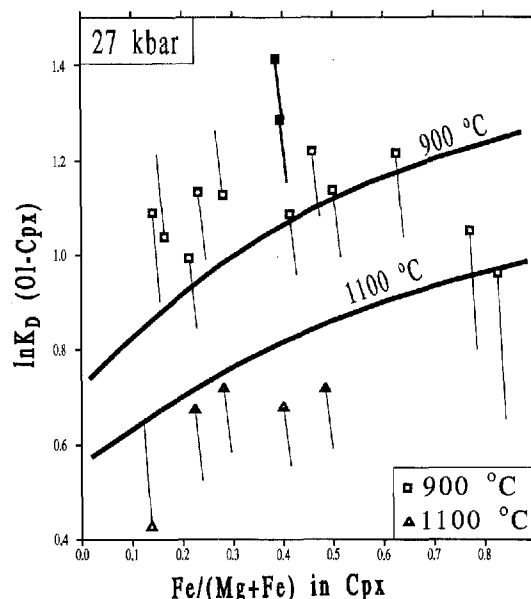


Fig. 2 Comparison of computed 27 kbar $\ln K_D$ curves at 900 and 1100 °C for equilibrium (B) with experimental data of Kawasaki and Ito (1993). Symbols as in Fig. 1, except that length of lines reflects 0.015 adjustments in the compositions of Ol and Cpx. Two inconsistent points at 900 °C are *highlighted in bold* and discussed in the text. Apparent discrepancies with two 900 °C half-brackets in Mg-rich compositions stem from fitting data with P, T uncertainties that are not shown

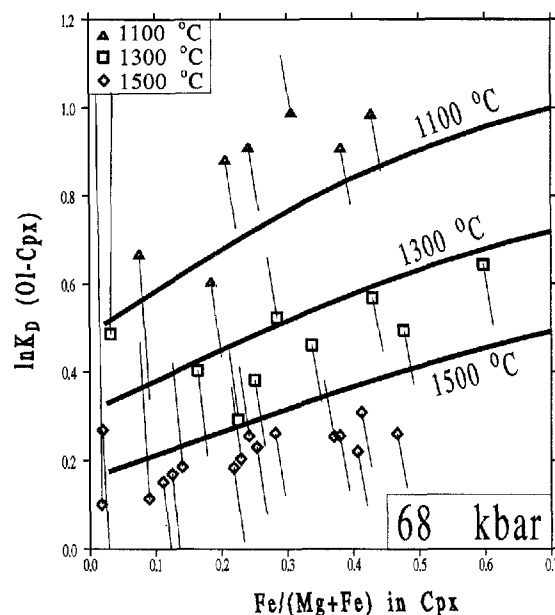


Fig. 3 Comparison of computed 68 kbar $\ln K_D$ curves at 1100, 1300, and 1500 °C for equilibrium (B) with experimental data of Kawasaki and Ito (1993). Symbols as in Fig. 2. All data are consistent with calculated curves if P, T uncertainties are accounted for.

patibilities, even when uncertainties in grossular content and Mg# of garnet in PN's experiments were accounted for. Use of an asymmetric model for Fe-Mg mixing on the M1 site of Cpx did not permit improvement

Table 3 Measured heterogeneities for starting and final garnets in selected PN runs

Run	$T^{\circ}\text{C}$	$P(\text{kbar})$	$100X_{\text{Gr}}$ Nominal Values	100 Mg#	$100X_{\text{Gr}}$ Measured Range ^a	100 Mg#
86b-2	800	15	20	14	17–25	10–18
76a-1	800	15	20	57	18–23	50–60
62b-2	900	15	20	57	18–23	50–60
69d	1100	15	20	14	17–25	10–18
61b	1100	15	20	29	17–23	23–33
70d	1200	15	20	29	17–23	23–33
4a	800	15	30	57	24–33	50–60
56a	1200	15	30	29	25–33	25–34
96b-1	800	15	50	57	41–65	50–63
97a-2	1000	15	50	21	48–54	18–23
82b-1	1000	15	30	57	24–33	50–60

^aRange of X_{Gr} and Mg# in either starting or final Grt, measured by PN or in part I. The Mg# range was used as compositional uncertainty in LIP analysis only for tabulated runs; the X_{Gr} range was used in addition only for runs 86b-2, 76a-1, 70d, and 4a.

in the overall representation of the combined data set. The inconsistencies could be resolved by deleting several PN runs (# 70d, 4a, 100d) or by modifying the minimum uncertainties applied to the KI data. The latter option appears more reasonable in the light of the limited discussion given by KI with respect to their determination of equilibrium compositions, which in some cases are tabulated with uncertainties as large as 0.02 (KI do not report whether these are 1 or 2 σ uncertainties). The modifications involved deleting one run (# KCH900912B), and expanding to 0.02 the compositional uncertainties applied to one run (# KCH9009125). These experiments, highlighted in bold in Fig. 2, are tabulated with standard errors in Cpx compositions of 0.018 and 0.02. With these changes, all PN experiments are consistent.

Having obtained a feasible solution for the entire experimental data set, we determined that a feasible solution could also be obtained with uncertainties in Grt compositions less than 0.03 Mg# for all but 11 of 137 PN experiments. For these 11 experiments, measured heterogeneities in Mg# were applied (see Table 3). For four of these 11 experiments (Table 3), heterogeneities in grossular content of starting garnets were also needed to obtain consistency with all other data. Taken at face value, we interpret these results to indicate that the most advanced Cpx compositions did equilibrate with the modally most abundant composition of starting garnets (see Part I for a description of the modal Mg# peaks) in most PN runs. For about 10% of the runs it appears that the most advanced clinopyroxene composition was in equilibrium with garnet removed from the nominal composition, but nevertheless within the range of the measured garnet compositions (Table 3).

The results summarized above are encouraging because they indicate that experimental data for equilibria (A-C) can be combined with reasonable estimates of overall experimental uncertainties, with few minor exceptions, to derive a consistent set of thermodynamic

properties for clinopyroxene, garnet, and olivine. Tables 4 and 5 give the thermodynamic parameters derived in this study. The experimental data set tightly constrain the standard free energy change of equilibrium (A) within the range -33.3 kJ/mol to -32.7 kJ/mol at 1000°C and 10.5 kbar. This range is slightly higher than the value derived by Perkins and Vielzeuf (1992), -29.3 ± 2.5 kJ/mol, based on combination of their free energy value for the O1-Cpx exchange equilibrium (B) with Hackler and Wood's (1989) free energy value for the O1-Grt exchange equilibrium (C). Our enthalpy change for equilibrium (A), -64.4 kJ/mol, is considerably larger, however, than that determined by Perkins and Vielzeuf (1992), -49.6 kJ/mol, due to differences in entropy values used in the two studies. The standard volume change of equilibrium (A) accepted in this study, -0.312 J/bar-mol, is based on cell refinements of synthetic end-member minerals. This value is larger than values determined experimentally by Ellis and Green (1979) and PN, but in better agreement with the results of the latter study.

Discussion

Figures 4 and 5 compare the PN data with computed $\ln K_D$ for equilibrium (A) as a function of Grt Mg/(Mg + Fe) for garnets with $X_{\text{Gr}} = 0.2$ and 0.3. An important feature found by PN and supported by our calculations (Figs. 4, 5), is that K_D decreases with increasing Mg# at all temperatures. Our calculations do not, however, support Pattison and Newton's (1989) interpretation that K_D also decreases with decreasing Mg# in the most Fe-rich compositions, even though this pattern is clearly suggested by their nominal data (e.g. 800–1100°C nominal data in Figs. 4, 5).

Perkins and Vielzeuf (1992) also deduced that K_D for equilibrium (A) has a strong compositional dependence on Mg/(Mg + Fe), but their dependence is the

Fig. 4 Comparison of computed 800°C–1200°C $\ln K_D$ curves for equilibrium (A) with experimental data of Pattison and Newton (1989). Curves and data pertain to 15 kbar and garnet with $X_{Gr} = 0.2$. Symbols as in Fig. 1, using 0.03 and 0.015 adjustments for the compositions of Grt and Cpx, respectively. All experimental data are consistent with the calculated curves when P - T uncertainties are accounted for, except for six experimental points (*dotted lines*) that require compositional adjustments equal to measured heterogeneity ranges (Table 3). The effect of heterogeneity in X_{Gr} is not shown. See text for discussion

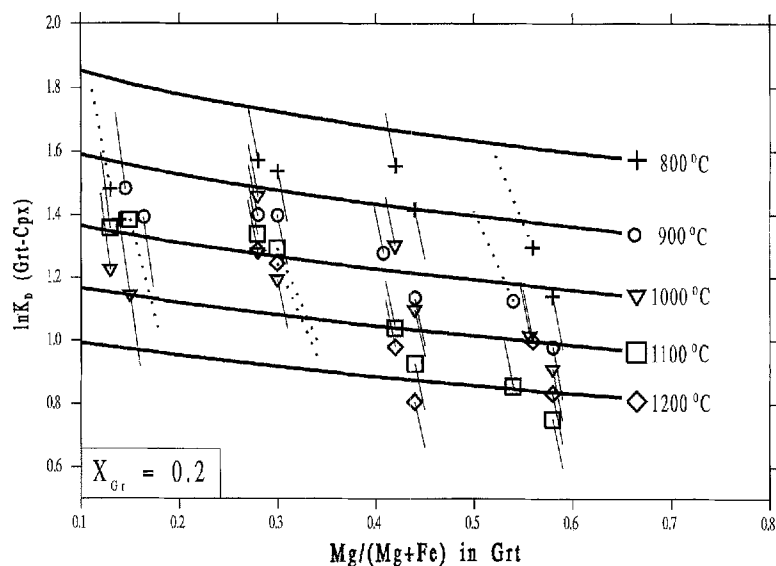
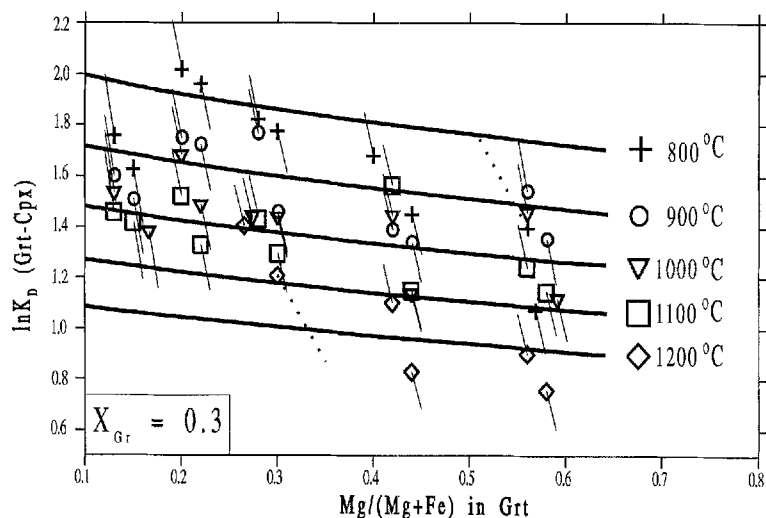


Fig. 5 Comparison of computed 800–1200°C $\ln K_D$ curves for equilibrium (A) with experimental data of Pattison and Newton (1989). Curves and data pertain to 15 kbar and garnet with $X_{Gr} = 0.3$. Symbols as in Fig. 4. All experimental data are consistent with the calculated curves, except for two experimental points (*dotted lines*) that require compositional adjustments equal to measured heterogeneity ranges (Table 3).



opposite of that described above. The dependence of K_D on $Mg/(Mg + Fe)$ is a function of the difference in nonideality on the Mg-Fe joins of Grt and Cpx, in addition to the difference between Ca-Mg and Ca-Fe interactions in Grt and Mg-Al and Fe-Al interactions in Cpx. The positive dependence of K_D on $Mg\#$ depicted by Perkins and Vielzeuf (1992) reflects their conclusion that nonideal Fe-Mg mixing is more positive in Cpx than in Grt. This conclusion rests on their fitting the Ol-Cpx data with a flatter slope (nominal data in Fig. 1) which requires that nonideality in Cpx be almost as positive as in Ol. PV derived $W_{12}^{Cpx} = 4.0 \pm 0.4$ kJ/atom, assuming Hackler and Wood's (1989) value of $W_{12}^{Ol} = 4.5 \pm 1.0$ kJ/atom (and $W_{12}^{Grt} = 1.6$ kJ/atom). The PN Grt-Cpx data, even when considered with realistic uncertainties, require that K_D for equilibrium (A) decreases with increasing

$Mg\#$ (Figs. 4, 5). This feature, which has also been observed recently by Ai (1994) in analysis of synthesis-type experiments on equilibrium (A), requires that nonideal Fe-Mg mixing in Cpx is less positive than in Grt.

Because of the correlation between mixing properties implicit in Eq. 3, consideration of data for any two of the equilibria (A-C) yield a fairly wide range of mixing properties for Cpx, Grt, and Ol. This range is greatly reduced when the data for all three linearly dependent equilibria are analysed simultaneously. Excess enthalpy of mixing in Ol, for example, can be as large as 5.3 kJ/atom with consideration of data for any two equilibria, while all data treated together constrain W_H^{Ol} between 1.25 and 1.75 kJ/atom. The latter values, as well as the Fe-Mg mixing parameters for Grt (Table 5), are about one-third the magnitude of those

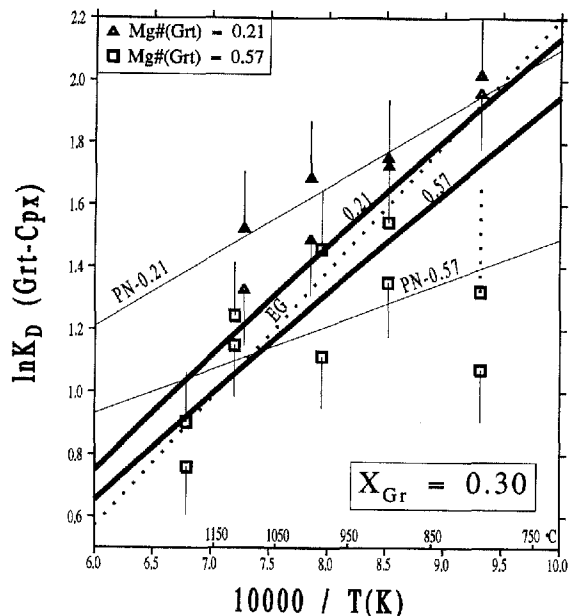


Fig. 6 Variation of $\ln K_D$ for equilibrium (A) with reciprocal temperature at 15 kbar. Heavy lines were computed with the data of Tables 4 and 5 for garnets with $X_{Gr} = 0.30$, $X_{py} = 0.21$ and 0.57 . Light solid lines and dashed line show $\ln K_D$ based on Pattison and Newton's (1989; PN) and Ellis and Green's (1979; EG) equations. Symbols as in Fig. 4. Symbols and PN curve adjusted to Al-free basis with Table 5 data

recommended by Hackler and Wood (1989). The asymmetry found for the Gr-Py join, which also causes K_D to decrease with increasing Mg#, is the opposite of that determined by heat of mixing measurements (Newton et al. 1977). Interpretation of recent phase equilibrium data on ternary Ca-Fe-Mg garnets yields the same sense of asymmetry as deduced in this study (Cheng and Ganguly 1991).

The mixing properties derived for Cpx yield small negative deviations from ideality over the temperature range 700–1300°C. The negative excess enthalpy and entropy (both symmetric) are reasonable for the assumption of equal partitioning of Fe-Mg between octahedral sites used in this study as the ideal reference. The affinity of Fe for Al is reflected in the 11.2 kJ/mol $W_{Mg-Al} - W_{Fe-Al}$ difference for the Cpx M1 site, a value in good agreement with that found for other silicates (Aranovich 1991; Mader and Berman 1992;

Table 5 Mixing parameters of solid solutions

Phase	Parameter	W_H (kJ/mol)	W_S (J/K·mol)	W_V (J/bar·mol)
Grt ^a	112	67.53	13.3	0.214
	122	43.04	13.3	0.017
	113	8.61	0.0	0.170
	133	3.40	0.0	0.090
	223	0.600	0.0	0.010
	233	1.81	0.0	0.060
Ol ^b	123	62.49	13.3	0.281
	12	3.00	0.00	0.045
Cpx ^c	12	-1.91	-1.05	0.000
	13-23	11.18	0.00	0.000

^a Grt: 1 = Ca, 2 = Mg, 3 = Fe. Ternary Grt mixing parameter for use with Eq. 6 represents one-half the sum of binary parameters (Berman 1990)

^b Ol: 1 = Mg, 2 = Fe

^c Cpx: 1 = Mg^{M1}, 2 = Fe^{M1}, 3 = Al^{M1}

Berman and Aranovich 1993). The effect of Al nonideality on the M1 site is to increase further the compositional dependence of K_D on Mg# over that shown in Figs. 4 and 5 which show the PN data recalculated to an Al-free Cpx basis.

Figure 6 summarizes the variation of $\ln K_D$ (Grt-Cpx) with reciprocal temperature for the new calibration presented here along with the calibrations of PN and Ellis and Green (1979; EG). Our curves (in bold) have slopes similar to, but slightly less steep than that of EG. The lower Mg# curve is displaced above and the higher Mg# curve below that of EG, which leads to higher and lower temperatures for these different bulk compositions. Overall the similarity of computed curves is quite remarkable considering that all of the experimental data obtained by EG were based on synthesis runs over a relatively small compositional range. The PN curves, fitted to their nominal data, have a much smaller slope which leads to lower temperature estimates for natural Cpx-Grt pairs. The surprisingly large difference between our slopes and PN's shows the significant effects of incorporating uncertainties of the PN experimental data.

Thermodynamic parameters given in Tables 4-5 can be used with Eq. 8 to compute Grt-Cpx temperatures for natural samples. Because thermodynamic data were derived using thermal expansivities and compressibilities of all minerals, we recommend the use of the quadratic equation (9) below that incorporates

Table 4 Standard reaction properties

#	Equilibrium	$\Delta_r H^0$ (kJ/mol)	$\Delta_r S^0$ (J/K·mol)	$\Delta_r V^0$ (J/bar·mol)
(A)	Grt-Cpx	-64.42	-25.99	-0.312
(B)	Ol-Cpx	-28.37	-10.96	-0.094
(C)	Ol-Grt	-43.74	-19.08	-0.342

these terms:

$$T = \frac{-b + \sqrt{b^2 - 4ac}}{2a} \quad (9)$$

where

$$a = 1.762 \times 10^{-7} (P - 1) \quad (9a)$$

$$b = 3R \ln K_D - \Delta_r S^0 - \Delta S_{\text{ex}} - 1.4017 \times 10^{-4} (P - 1) \quad (9b)$$

$$c = \Delta_r H^0 + \Delta H_{\text{ex}} + (P - 1)(\Delta_r V^0 + \Delta V_{\text{ex}} + 2.613 \times 10^{-2}) \\ + 4.0335 \times 10^{-7} P^2 + 4.7 \times 10^{-12} P^3 \quad (9c)$$

with T in Kelvins and P in bars.

Uncertainties in temperatures (σ_T) calculated with Eq. 9 are difficult to assess quantitatively, and several recent publications (e.g. Aranovich 1991; Kohn and Spear 1991; Hodges and McKenna 1987; Powell 1985b; Powell and Holland 1988) have addressed the problem of error propagation in geothermobarometry. Uncertainties in temperature estimates can be attributed to uncertainties in calibration (σ_{T_c}) and in mineral analyses (σ_{T_a}), in addition to the erroneous assumption that the compositions used for coexisting minerals were in equilibrium (e.g. Hodges and McKenna 1987; Kohn and Spear 1991). To evaluate the uncertainties related to calibration of the garnet-clinopyroxene geothermometer (σ_{T_c}), it is necessary to estimate the uncertainties of the derived thermodynamic parameters. The LIP method does not explicitly provide such estimates, although one can obtain a range of parameter values consistent with the experimental data base (e.g. Berman et al. 1986; Andersen et al. 1991; Patino Douce et al. 1993). As a first approximation we assumed that 2σ uncertainties of thermodynamic properties of equilibrium (A) were equal to half the difference between maximum and minimum values determined ($-58.94 > \Delta_r H^0 > -64.84$ kJ/mol; $-26.3 < \Delta_r S^0 < -21.8$ J/K·mol). LIP runs performed with different optimization schemes show strong correlation between derived parameters. For example, the maximum standard enthalpy change of equilibrium (A) is accompanied by the maximum entropy change. This correlation, well known from calibration of exchange geothermometers with regression techniques (Powell 1985a; Aranovich 1991; von Seckendorff and O'Neill 1993), reflects the fact that even for equilibria studied over a wide temperature and compositional range, such as that considered here, the Gibbs free energy of reaction is constrained much better than $\Delta_r H^0$, $\Delta_r S^0$, and W terms separately. Assuming complete correlation between these terms, and $2\sigma_{\Delta_r H} = 2.95$ kJ/mol, we calculate $2\sigma_{T_c} = 42\text{--}56^\circ\text{C}$ for the temperature range $700\text{--}850^\circ\text{C}$ and garnet $\text{Mg}\# = 0.2\text{--}0.5$. Assuming optimistically that $2\sigma_{T_a} = 10^\circ\text{C}$ (Kohn and Spear 1991) gives $2\sigma_T = 43\text{--}57^\circ\text{C}$ for application of Eq. 9 to “normal” bulk compositions. We feel this estimate pro-

vides an upper bound because the present results are based on experimental data for a linearly dependent set of phase equilibria with conservative uncertainty adjustments (see discussion of PN data above, and Table 2), and because of the incorporation of thermodynamic constraints on end-members and mixing properties of Grt, Cpx, and O1. Support for this conclusion comes from comparison of temperatures calculated for the samples in Table 6 using sets of parameters corresponding to the minimum and maximum $\Delta_r H^0$ values discussed above. For most compositions, computed temperatures differ from that calculated with the preferred set of parameters by less than $15\text{--}20^\circ\text{C}$. For Fe-rich and Gr-rich samples these differences are up to 30°C .

In order to test the calibration, the TWQ software (Berman 1991) was used to calculate the equilibration temperatures for a large number of Grt-Cpx samples that span three main metamorphic facies typical for this assemblage: lower to intermediate amphibolite (Ghent et al. 1983), amphibolite-granulite transition (Percival 1983), and granulite (Coolen 1980). For each terrain, calculated temperatures (Table 6) show a range that in all cases is smaller than that obtained with the calibration of PN, and quite similar to that produced with the EG formulation. Nevertheless, the nontrivial range within each area suggests that errors related to calibration, disequilibrium, or retrograde exchange are not entirely absent. Most significant is the finding that computed temperatures are generally about $70\text{--}200^\circ\text{C}$ higher than obtained with the calibration of PN, showing the important effects of incorporating experimental uncertainties in modelling the PN data. These computed temperatures are in more reasonable agreement with independent T estimates, where these are available, and are similar to those reported by Perkins and Vielzeuf (1992).

Several features of Table 6 are worthy of further comment. Particularly encouraging is the good agreement between independent estimates of Adirondack Highland temperatures and computed temperatures for extremely Fe-rich garnets ($X_{\text{Fe}}^{\text{Grt}} = 0.98\text{--}0.99$) reported by Jaffc et al. (1978), suggesting that this calibration is applicable to a wide range of bulk compositions. Temperatures computed for the Kapuskasing rocks average about 25°C lower than the EG calibration, a difference that leads to approximately 1 kbar lower calculated pressures for this extremely well studied terrain. The 725°C average temperature (Table 6) is compatible with the occurrence of tonalitic leucosome in mafic gneisses, although lower than expected for their origin by dehydration melting (Hartel 1993). Temperatures computed for 5 Mica Creek samples (those discussed by PN) are between $634\text{--}722^\circ\text{C}$, in comparison to $570\text{--}654^\circ\text{C}$ and $701\text{--}780^\circ\text{C}$ for the PN and EG calibrations, respectively. Our temperature estimates for these rocks are in better agreement with the presence of muscovite-sillimanite-K feldspar-bearing migmatites in adjacent pelitic samples.

Table 6 Temperatures (°C) computed for selected Grt-Cpx assemblages

Locality	# ^a	100X _{Py}	Range -This paper-	Avg	Rang --EG--	Avg	Range --PN--	Avg	Estimate	Author
Mica Creek, British Columbia	7	11-18	634-722	681	700-780	731	470-654	549	650	Ghent et al. (1983)
Kapusksasing, Ontario ^b	27	13-43	636-809	717	649-847	744	460-790	626	700-750	Percival (1983)
	23	13-43	686-782	725	689-814	751	596-677	633		
Adirondack Highlands	2	1-2	717-788	753	674-735	705	n/a ^c		750-800	Jaffe et al. (1978)
Adirondack Highlands	10	16-51	693-828	757	711-857	785	504-643	578	750-800	Johnson & Essene (1982)
Furua Complex, Tanzania	18	25-41	698-923	802	724-970	819	570-853	707	800	Coolen (1980)
	14	29-40	783-848	814	797-870	828	632-782	718		

^a # = Number of samples used

^b Excluding skarn sample

^c n/a = beyond compositional limit of applicability (Pattison and Newton 1989)

Ghent et al. (1983) found that temperatures computed with the EG calibration were in best agreement with independent estimates when Fe³⁺ was accounted for in Grt and Cpx. Our calculations with Eq. 9 indicate better agreement with all Fe as Fe²⁺, a result which suggests similar oxidation states for the natural samples and the experimental run products on which Eq. 9 is based. This is supported by similar calculated Fe³⁺ contents in Ghent et al.'s natural metabasites (0.05-0.12) compared to the experimental run products of PN (Table 1 of Part 1). We have also observed less scattered results for all other localities listed in Table 6 when all iron is assumed to be Fe²⁺, presumably because of the sensitivity of calculated Fe³⁺ to microprobe analytical errors. For this reason we advise applying Eq. 9 with all Fe as Fe²⁺, unless there is strong evidence that samples are highly oxidized. For example, Grt-Cpx from a Kapuskasing skarn (Percival 1983) yields a much lower (550°C) temperature than other bulk compositions when all Fe is considered as Fe²⁺.

Conclusions

Thermodynamic analysis has revealed that the experiments of Pattison and Newton (1989), reevaluated in Part I of this study, are consistent with other phase equilibrium data involving garnet, clinopyroxene, and olivine, as well as thermophysical data on individual phase properties, if realistic estimates of uncertainties, consistent with experimental procedures, are applied to the PN data.

Temperature estimates based on the derived Grt-Cpx thermodynamic properties are generally 70-200°C higher than those obtained by Pattison and Newton (1989), and are more compatible with temperature estimates based on other Fe-Mg exchange equi-

libria (Grt-Opx, Grt-Bi; c.g. Aranovich 1991). Whether the use of carefully selected and analyzed Grt-Cpx pairs yield near-peak or significantly reset temperatures, however, is a question that requires detailed analysis of zoning patterns and assessment of results against constraints from quantitative petrogenetic grids and/or net transfer equilibria (e.g. Anovitz 1991; Pattison and Begin 1994).

We emphasize that the thermodynamic parameters and geothermometer derived in this study are provisional in nature. In order to have more confidence in the derived thermodynamic properties, analysis is needed of a larger experimental data set capable of further constraining thermodynamic properties of Grt and Cpx. Additional experimental study focusing on the compositions listed in Table 3 would also be very useful in order to test the conclusions of this study.

Acknowledgements We thank Dexter Perkins and Toshisuke Kawasaki for sharing their experimental results with us prior to their publication. We are also grateful to the Continental Geoscience Division of the Geological Survey of Canada and NSERC for the support LYA has received for part of 1991 and 1992. Helpful reviews by Larry Anovitz, Bob Newton, John Percival, and Dexter Perkins are greatly appreciated. This is Geological Survey of Canada contribution no. 50494.

References

- Ai Y (1994) A revision of the garnet-clinopyroxene Fe²⁺-Mg exchange geothermometer. *Contrib Mineral Petrol* 115:467-473
- Andersen DJ, Bishop FC, Lindsley DH (1991) Internally consistent solution models for Fe-Mg-Mn-Ti oxides: Fe-Mg-Ti oxides and olivine. *Am Mineral* 76:427-444
- Anovitz LM (1991) Al-zoning in pyroxene and plagioclase: window on late prograde/early retrograde P-T Paths in granulite terranes. *Am Mineral* 76:1328-1343
- Aranovich LY (1983) Biotite-garnet equilibria in metapelites: I. Thermodynamics of solid solutions and end-member reactions. *Ocherki Phys Chem Petrol* XI: 121-136
- Aranovich LY (1991) Mineral equilibria of multicomponent solid solutions (in Russian). Nauka Press, Moscow

- Aranovich LY, Pattison DRM (1995) Reassessment of the garnet-clinopyroxene Fe-Mg exchange thermometers: I. Evaluation of the Pattison and Newton (1989) experiments. *Contrib Mineral Petrol* 119:16–29
- Berman RG (1988) Internally-consistent thermodynamic data for stoichiometric minerals in the system $\text{Na}_2\text{O}-\text{K}_2\text{O}-\text{CaO}-\text{MgO}-\text{FeO}-\text{Fe}_2\text{O}_3-\text{Al}_2\text{O}_3-\text{SiO}_2-\text{TiO}_2-\text{H}_2\text{O}-\text{CO}_2$. *J Petrol* 29:445–522
- Berman RG (1990) Mixing properties of Ca-Mg-Fe-Mn garnets. *Am Mineral* 75:328–344
- Berman RG (1991) Thermobarometry using multi-equilibrium calculations – a new technique, with petrological applications. *Can Mineral* 29:833–855
- Berman RG, Aranovich LY (1993) Optimized standard state and solution properties of olivine, orthopyroxene, cordierite, garnet, and biotite. *Geol Soc Am Abstr Progr* 25:A-100
- Berman RG, Engi M, Greenwood HJ, Brown TH (1986) Derivation of internally consistent thermodynamic properties by the technique of mathematical programming, a review with application to the system $\text{MgO}-\text{SiO}_2-\text{H}_2\text{O}$. *J Petrol* 27:1331–1364
- Bohlen SR, Essene FJ, Boettcher AL (1980) Reinvestigation and application of olivine-quartz-orthopyroxene barometer. *Earth Planet Sci Lett* 47:1–10
- Bohlen SR, Lioy JJ (1986) A barometer for garnet amphibolites and garnet granulites. *J Petrol* 27:1025–1034
- Bohlen SR, Wall WJ, Boettcher AL (1983a) Experimental investigations and geological applications of equilibria in the system $\text{FeO}-\text{TiO}_2-\text{Al}_2\text{O}_3-\text{SiO}_2-\text{H}_2\text{O}$. *Am Mineral* 68:1049–1058
- Bohlen SR, Wall VJ, Boettcher AL (1983b) Experimental investigation and application of garnet granulite equilibria. *Contrib Mineral Petrol* 83:52–61
- Brey GP, Kohler T (1990) Geothermobarometry in four-phase lherzolites II. New thermobarometers, and practical assessment of existing thermobarometers. *J Petrol* 31:1353–1378
- Brown GE, Prewitt CT, Papike JJ, Sueno S (1972) A comparison of the structures of low and high pigeonite. *J Geophys Res* 77:5778–5789
- Carlson WD, Lindsley DH (1988) Thermochemistry of pyroxenes in the join $\text{Mg}_2\text{Si}_2\text{O}_6-\text{CaMgSi}_2\text{O}_6$. *Am Mineral* 73:242–252
- Cheng W, Ganguly J (1991) Some binary and ternary mixing relations in (Fe, Mg, Ca, Mn) garnets. *EOS Trans Am Geophys Union* 72:565
- Coolen JJM (1980) Chemical petrology of the Furua granulite complex, southern Tanzania. *GUA Pap Geol* 13:1–258
- Dahl PS (1980) The thermal-compositional dependence of Fe^{2+} - Mg^{2+} distributions between coexisting garnet and pyroxene: applications to geothermometry. *Am Mineral* 65:852–866
- Davidson PM, Lindsley DH (1985) Thermodynamic analysis of quadrilateral pyroxenes. Part II. Model calibration from experiments and applications to geothermometry. *Contrib Mineral Petrol* 80:88–102
- Ellis DJ, Green DH (1979) An experimental study of the effect of Ca upon garnet-clinopyroxene Fe-Mg exchange equilibria. *Contrib Mineral Petrol* 71:13–22
- Frost BR, Chacko T (1989) The granulite uncertainty principle: limitations on thermobarometry in granulites. *J Geol* 97:435–450
- Ganguly J (1979) Garnet and clinopyroxene solid solutions, and geothermometry based on Fe-Mg distribution coefficient. *Geochim Cosmochim Acta* 43:1021–1029
- Ganguly J, Saxena SK (1984) Mixing properties of aluminosilicate garnets: constraints from natural and experimental data, and applications to geothermo-barometry. *Am Mineral* 69:88–97
- Geiger CA, Newton RC, Kleppa OJ (1987) Enthalpy of mixing of synthetic almandine-grossular and almandine-pyroxene garnets from high-temperature solution calorimetry. *Geochim Cosmochim Acta* 51:1755–1763
- Ghent ED, Stout MZ, Raeside RP (1983) Plagioclase-clinopyroxene-garnet-quartz equilibria and the geobarometry of garnet amphibolites from Mica Creek, British Columbia. *Can J Earth Sci* 20:699–706
- Green TH, Adam J (1991) Assessment of the garnet clinopyroxene Fe-Mg exchange thermometer using new experimental data. *J Metamorphic Geol* 9:341–347
- Hackler RT, Wood BJ (1989) Experimental determination of Fe and Mg exchange between garnet and olivine and estimation of Fe-Mg mixing properties in garnet. *Am Mineral* 74:994–999
- Hartel THD (1993) Genesis of mafic migmatites from the Kapuskasing Structural Zone, Ontario, Canada. MSc thesis, Univ of Calgary, Alberta
- Hodges KV, McKenna LW (1987) Realistic propagation of uncertainties in geologic thermobarometry. *Am Mineral* 72:671–680
- Jaffe HW, Robinson P, Tracy RJ (1978) Orthoferrosilite and other iron-rich pyroxenes in micropertthite gneiss of the Mount Marcy area, Adirondack Mountains. *Am Mineral* 63:1116–1136
- Johnson CA, Essene EJ (1982) The formation of garnet in olivine-bearing metagabbros from the Adirondacks. *Contrib Mineral Petrol* 81:240–251
- Kawasaki T, Ito E (1993) Fe-Mg partitionings between olivine-Ca-rich clinopyroxene: implications for Fe-Mg mixing properties of Ca-rich clinopyroxene. Tech Report ISEI, Okayama Univ 54
- Kohn MJ, Spear FS (1991) Error propagation for barometers: 2. Application to rocks. *Am Mineral* 76:128–137
- Koziol AM (1990) Activity-composition relationships of binary Ca-Fe and Ca-Mn garnets determined by reversed, displaced phase equilibrium experiments. *Am Mineral* 75:319–327
- Koziol AM, Bohlen SR (1992) Solution properties of almandine-pyroxene garnet as determined by phase equilibrium experiments. *Am Mineral* 77:765–773
- Lee HY, Ganguly J (1988) Equilibrium compositions of coexisting garnet and orthopyroxene: experimental determinations in the system $\text{FeO}-\text{MgO}-\text{Al}_2\text{O}_3-\text{SiO}_2$, and applications. *J Petrol* 29:93–113
- Mader UK, Berman RG (1992) Amphibole thermobarometry: a thermodynamic approach. *Current Res Geol Surv Can* 92-1E:393–400
- McCallister RH, Finger LW, Ohashi Y (1976) Intracrystalline Fe^{2+} -Mg equilibria in three natural Ca-rich clinopyroxenes. *Am Mineral* 61:671–676
- Newton RC (1983) Geobarometry of high-grade metamorphic rocks. *Am J Sci* 283-A:1–28
- Newton RC, Charlu TV, Kleppa OJ (1977) Thermochemistry of high pressure garnets and clinopyroxenes in the system $\text{CaO}-\text{MgO}-\text{Al}_2\text{O}_3-\text{SiO}_2$. *Geochim Cosmochim Acta* 41:369–377
- Patino Douce AE, Johnston AD, Rice JM (1993) Octahedral excess mixing properties in biotite: a working model with applications to geobarometry and geothermometry. *Am Mineral* 78:113–131
- Pattison DRM (1994) Are “reversed” Fe-Mg exchange and solid solution experiments really reversed? *Am Mineral* 79:938–950
- Pattison DRM, Begin NJ (1994). Zoning patterns in orthopyroxene and garnet in granulites: implications for geothermometry. *J Metamorphic Geol* 12:387–410
- Pattison DRM, Newton RC (1989) Reversed experimental calibration of the garnet-clinopyroxene Fe-Mg exchange thermometer. *Contrib Mineral Petrol* 101:87–103
- Perchuk LL (1969) Garnet-clinopyroxene equilibrium as an indicator of temperature of deep-scated rocks. *Izvestiya Acad Nauk USSR* 6:144–169
- Percival JA (1983) High-grade metamorphism in the Chapleau-Foley Area, Ontario. *Am Mineral* 68:667–686
- Perkins D, Vielzeuf D (1992) Experimental investigation of Fe-Mg distribution between olivine and clinopyroxene: implications for mixing properties of Fe-Mg in clinopyroxene and garnet-clinopyroxene thermometry. *Am Mineral* 77:774–783
- Perkins D, Holland TJB, Newton RC (1981) The Al_2O_3 contents of enstatite in equilibrium with garnet in the system $\text{MgO}-\text{Al}_2\text{O}_3-\text{SiO}_2$ at 15–40 kbar and 900–1600°C. *Contrib Mineral Petrol* 78:99–109

- Powell R (1985a) Regression diagnostics and robust regression in geothermometer/geobarometer calibration: the garnet-clinopyroxene geothermometer revisited. *J Metamorphic Geol* 3:231–243
- Powell R (1985b) Geothermometry and geobarometry: a discussion. *J Geol Soc London* 142:29–38
- Powell R, Holland TJB (1988) An internally consistent dataset with uncertainties and correlations: 3. Applications to geobarometry, worked examples and a computer program. *J Metamorphic Geol* 6:173–204
- Råheim A, Green DH (1974) Experimental determination of the temperature and pressure dependence of the Fe-Mg partition coefficient for coexisting garnet and clinopyroxene. *Contrib Mineral Petrol* 48:179–203
- Sack RO, Ghiorso MS (1989) Importance of considerations of mixing properties in establishing an internally consistent thermodynamic database: thermochemistry of minerals in the system Mg_2SiO_4 - Fe_2SiO_4 - SiO_2 . *Contrib Mineral Petrol* 102:41–68
- Sack RO, Ghiorso MS (1994) Thermodynamics of multicomponent pyroxenes: II. Phase relations in the quadrilateral. *Contrib Mineral Petrol* 116:277–286
- Saxena SK (1979) Garnet-clinopyroxene geothermometer. *Contrib Mineral Petrol* 70:229–235
- Saxena SK, Ghose S, Turnock AC (1974) Cation distribution in low-calcium pyroxenes: dependence on temperature and calcium content and the thermal history of lunar and terrestrial pigeonites. *Earth Planet Sci Lett* 21:194–200
- von Seckendorff V, O'Neill HSC (1993) An experimental study of Fe-Mg partitioning between olivine and orthopyroxene at 1173, 1273, and 1423 K and 1.6 Gpa. *Contrib Mineral Petrol* 113:196–207
- Wiser NM, Wood BJ (1991) Experimental determination of activities in Fe-Mg olivine at 1400 K. *Contrib Mineral Petrol* 108:146–153
- Wood BJ (1988) Activity measurements and excess entropy-volume relationships for pyrope-grossular garnets. *J Geol* 96:721–729